Article:

Numan Kaya, M., Kose, F., Ma, L. et al. (1 more author) (2018) Aerodynamic performance of a horizontal axis wind turbine with forward and backward swept blades. Journal of Wind Engineering & Industrial Aerodynamics, 176. pp. 166-173. ISSN 0167-6105

https://doi.org/10.1016/j.jweia.2018.03.023

AERODYNAMIC PERFORMANCE OF A HORIZONTAL AXIS WIND TURBINE WITH FORWARD AND BACKWARD SWEPT BLADES

Mehmet Numan Kaya[a,b,c,*], Faruk Kose[b], Derek Ingham[a], Lin Ma[a], Mohamed Pourkashanian[a]

[a] University of Sheffield, Department of Mechanical Engineering, Energy2050 Research Group, Sheffield, UK
[b] Selcuk University, Engineering Faculty, , Department of Mechanical Engineering, Konya, Turkey
[c] Necmettin Erbakan University, Engineering and Architecture Faculty, Department of Mechanical Engineering, Konya, Turkey

Abstract

Blades are the most important components of wind turbines in order to convert wind energy to mechanical energy. This study investigates the aerodynamic performance of Horizontal Axis Wind Turbines (HAWTs) with forward and backward swept blades. The effect of the blade sweep direction, the location of the sweep start up and the tip offset on the aerodynamic performance are investigated using a model HAWT with a 0.9 m rotor as the baseline configuration. Changes in power and thrust coefficients with swept blades are investigated for the design tip speed ratio of the baseline wind turbine at a wind speed of 10 m/s. The wind turbine with the forward swept blade that has sweep start up at $r_{ss}/R=0.15$ and tip offset of d/D=0.2 has been found to give a remarkable boost to the power output with an increase of about 2.9% over the baseline turbine. The backward swept blade with $r_{ss}/R=0.75$ and d/D=0.2 has shown the highest reduction in thrust coefficient, namely 5.4%, at the design tip speed ratio. In conclusion, it is found that the forward swept blades have the ability of increasing the performance while the backward swept blades tend to decrease the thrust coefficient.

Keywords

Swept blade, Horizontal axis wind turbine, Aerodynamics, CFD, Power coefficient

1. Introduction

Wind energy is one of the most utilized leading renewable energy sources for sustainable power production (REN21, 2017). Commercially, horizontal axis wind turbines (HAWTs) dominate the market and they are mostly preferred by the investors. Aerodynamic design of the turbine blades is very crucial in order to capture the wind and convert it to mechanical power efficiently (IRENA, 2012). Hence, increasing the aerodynamic efficiency of HAWT blades has always been a popular topic in the literature and the Computational Fluid Dynamics (CFD) method has been widely used in these studies (El-Farra et al., 2014; Kartheikeyan et al., 2014; Larin et al., 2016, Moshfeghi et al., 2017). For instance, Jafari and Kosasih (2014) investigated various diffuser augmented wind turbine designs and changes in aerodynamic efficiencies according to the diffuser length and area using CFD method. Bai et al. (2013) designed a 10 kW horizontal axis wind turbine blade and performed an aerodynamic investigation using a numerical simulation approach. They reported that CFD is a good method compared to the improved BEM theory method on the aerodynamic investigation of HAWT blades. As stated before, there are numerous studies on horizontal axis wind turbine blade designs but there are only a few on swept blades. A 54 m diameter rotor with backward swept horizontal axis wind turbine blades was designed

*Corresponding author. M.N. Kaya
E-mail address: mnkaya@konya.edu.tr

and compared with a field test by the Sandia National Laboratories of the US Energy Department (Ashwill et al., 2010). Investigation results for the Sweep Twist Adaptive Rotor (STAR) blades are presented by Ashwill (2010) and it is stated that the STAR technology provided a greater energy capture compared to the baseline 48 m diameter rotor straight-bladed wind turbine without incurring higher operating loads on the turbine. Khalafallah et al. (2015) performed a CFD study to investigate the sweep direction and start up location that affect the performance of HAWTs with swept blades and they concluded that some performance increase can be achieved when using swept blades. Amano et al. (2013) investigated backward swept blades and stated that at lower wind speeds the backward swept blades give better performance whereas at higher wind speeds they give lower power outputs compared to the straight blades. Different blade tip modifications have been considered and analysed independently with an optimization code, based on the Goldstein vortex model by Chattot (2009). The author of this study compared the design of a rotor blade with a straight, ±10% (forward or backward) sweep, dihedral and winglet and concluded that the aerodynamic performance is, in general, enhanced by these tip modifications, although the trends differ between the forward and backward orientations. Shen et al. (2016) studied an aerodynamic shape optimization of non-straight small wind turbine blades where they attempted to optimize the annual energy production and the starting performance of HAWTs. According to these results, the wind turbine blades with a properly designed 3- dimensional stacking line can increase the annual energy production and have a better starting behaviour. Verelst and Larsen (2010) and Hansen (2011) have performed studies that are mainly focused on the blade loads of swept horizontal axis wind turbine blades, where both used a 5 MW NREL wind turbine as a baseline. The findings of both studies were that the backward swept blades present slightly lower power outputs while presenting reduced loadings on the blade, tower and shaft in general. Generally, previous studies on HAWTs with swept blades were focused on blade loads. Moreover, none of the previous studies investigated the effect of both the blade tip offset and the sweep start up section on the aerodynamic performance.

This study investigates the aerodynamic performance of wind turbines with various forward and backward swept blades using CFD. The blade sweep is applied in the plane of the rotor and the swept blades are designed according to the various sweep start up sections and tip offsets. An equation that allows both the change in the sweep start up section and tip offset has been developed to calculate the offset at each blade section from the pitchline. The Norwegian University of Science and Technology (NTNU) wind turbine is used as the baseline wind turbine and the CFD method used is validated against the experimental results of this wind turbine.

2. Baseline Blade and Newly Designed Swept Blades

The model HAWT designed at the NTNU has a three bladed rotor and uses the NREL S826 airfoil throughout the blade span. The wind turbine has a 0.9 m rotor diameter, zero pitch angle and a hub diameter of 0.09 m. The design tip speed ratio of the blade was λ=6. Sketches of the NTNU wind turbine blades are given in Fig. 1, where the full rotor is illustrated as well. Full details of the wind turbine can be found in the study by Krogstad and Lund (2012).

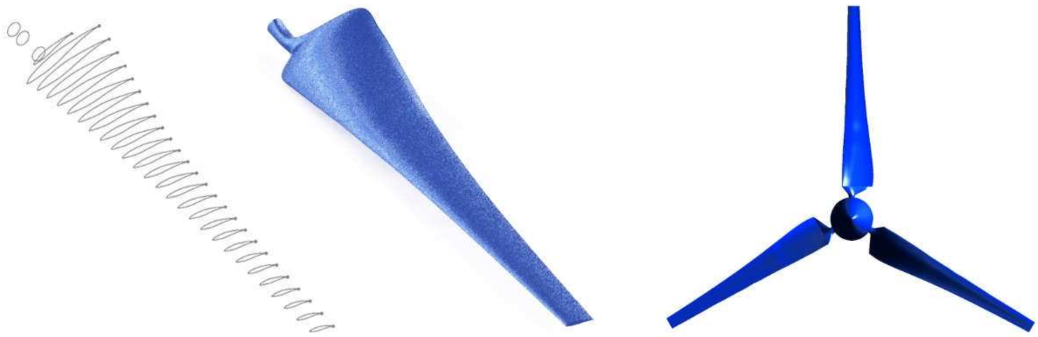

Fig. 1. 3D sketches of the baseline blade.

Regarding the swept blade design, although there are various equations available in the literature to calculate offset of each section of the blade from the pitchline (Ashwill, 2010, Amano et al., 2013; Hansen, 2011; Verelst and Larsen, 2010), it was not possible to change the tip displacement using these equations. Hence, an equation that makes it possible to select the tip offset, sweep start up and strength of the sweep is developed in order to calculate the offset from the pitchline at each blade section as follows:

$$z_{\text{offset}} = \frac{\left(r_r - r_{ss}\right)\left(R \times P_s\right) / \left(R - r_{ss}\right)}{M^{\left((1-P_{\mathrm{r}})(1-P_{rss})/P_{\mathrm{r}}\right)}} \tag{1}$$

where, z_{offset} is the offset of the blade section from the pitchline, r_r is the radial distance of the section (m), r_{ss} is the radial distance of the sweep start section, R is the blade radius, P_s is the ratio of the tip offset to the blade radius ($P_s = d/R$), M is the mode of the sweep, P_r is the ratio of the radial distance to the blade radius ($P_r = r_r/R$) and P_{rss} is the ratio of the radial distance of the sweep start up to the blade radius ($P_{rss}=r_{ss}/R$). The mode of the sweep (M) defines the strength of the sweep, increase in this value reduces the sweeping strength whereas decreasing the value close to one increases the strength of the sweep. This values is selected as M=2 since it likely represents an average sweep strength. In Equation (1), $R \times P_s$ gives the $z_{\text{offset,tip}}$ which is the offset at the tip of the blade. To test the effect of the swept blades on the power performance, four sweep start up sections and four tip offsets are selected as given in Table 1.

Table 1

Newly designed swept blades.

Direction	Sweep start up (r_{ss}/R)	Tip offset (d/R)
Forward	0.15	0.05
	0.35	0.10
Backward	0.55	0.15
	0.75	0.20

In total, 32 wind turbine blades, 16 forward swept and 16 backward swept, are designed and sketches of all the blades are illustrated in Fig. 2. As it can be seen from the figure, forward swept blades are swept in the direction of the rotation direction whereas backward swept blades have sweep in the opposite direction.

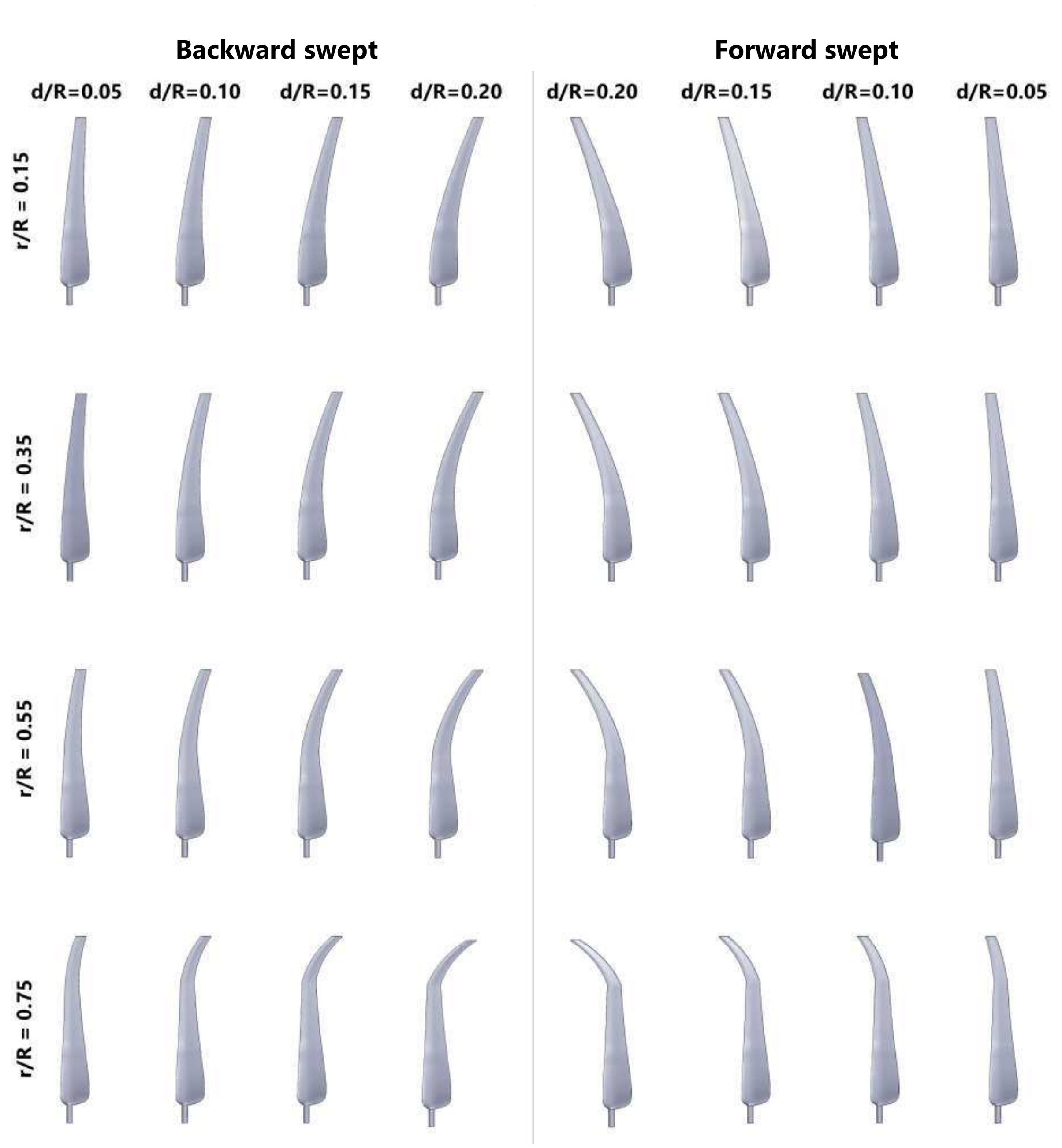

Fig. 2. Sketches of the designed swept blades.

3. CFD Methodology and Validation

In this study, the 3-D air flow around the wind turbine blade is simulated using the ANSYS Fluent 17.2 software in a moving reference frame. The dimensions of the flow field are similar to the wind tunnel located in the Norwegian University of Technology. The upstream and downstream boundaries of the fluid computational domain are 4.5D and 7.8D, respectively (D is the rotor diameter). Only one third of the rotor is used in the CFD simulations with rotational periodic conditions applied and to benefit from the periodic boundary condition the walls of the wind tunnel are defined to be circular with the same cross-sectional area as in the wind tunnel test section. This methodology has been used in several CFD simulation studies of HAWTs (Krogstad and Lund, 2012; Sørensen et al. 2002). The SIMPLE scheme is used for the calculations whereas the second-order interpolation scheme for the pressure, the second-order upwind discretization scheme for the momentum and turbulence equations were used.

Meshing of the fluid domain is performed using ANSYS meshing. The thickness of the first cell to the blade surface was kept at 1 x 10^{-5} m in order to keep the y+ value around 1 to have the confidence that the enhanced wall treatment was suitable for the grid (Krogstad and Lund, 2012). The y+ value reached its maximum value of almost 2 near the tip of blade and it was mostly around 1 in the other regions of the blade. Some pictures of the grid on the blade are presented in Fig. 3.

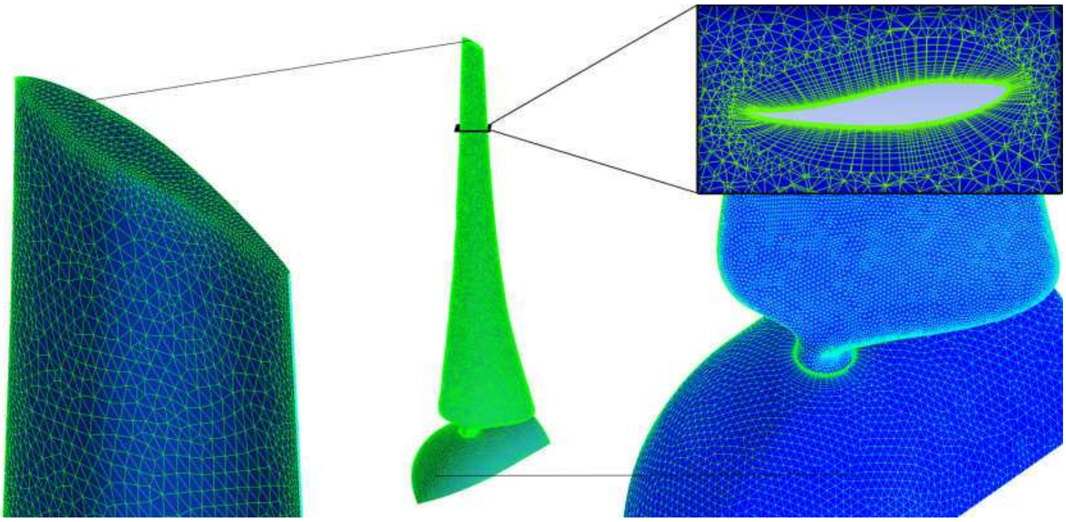

Fig. 3. Some pictures of the grid on the blade.

For the grid independence study, both the k-ω SST and k-ε Realizable models were used. A mesh independence study was performed for various models containing a different number of mesh elements. Details of the grids and the resulting power coefficients are presented in Table 2 where it is observed that the results do not significantly change after employing more than 4.8 million elements. Hence, a grid that has about 4.8 million elements has been used in the current study. Although this is an expensive grid to use, it was used in order to have confidence in the power and thrust coefficients. Moreover, it should be noted that making the value of y+ suitable for enhanced wall treatment dramatically increases the mesh element number. For the swept blades, the same sizing functions are used for the mesh and it is ensured that all the setups have similar element numbers. The maximum difference in the cell numbers between the baseline and swept blades was about 3%. As for the boundary conditions, the top surface domain is defined as a wall so as to mimic the wind tunnel wall and the inlet is defined as a velocity inlet with a constant wind speed of 10 m/s and the flow outlet is defined as a pressure outlet with a constant pressure. The turbulent intensity at the inlet is defined to be 0.3%, as provided for the wind tunnel used for the experimental tests (Krogstad and Lund, 2012). The convergence criterion is set to achieve a reduction in all scaled residuals below the value of 10^{-4}. In addition, it is ensured that the monitored torque and thrust force on the blade shows no further change. All the simulations were performed on the High Performance Computing facilities of the

University of Sheffield where in general, Intel E5-2630 V3 processors were used for the simulations and the time spent for each simulation was almost 8 hours when using 8 cores.

Table 2
Mesh independency study.

Number of elements ($x10^6$)	**Number of nodes ($x10^6$)**	**C_p at λ=6 k-ε Realizable**	**C_p at λ=6 k- ω SST**
2.2	0.9	0.4344	0.4303
3.5	1.52	0.4391	0.4376
4.8	2.02	0.4448	0.4437
6.5	2.73	0.4456	0.4454

In order to validate the CFD method used, the CFD results are compared with the available experimental data (Krogstad and Lund, 2012) for the power coefficient (C_p) and the thrust coefficient (C_t), as a function of the tip speed ratio (λ), and they are presented in Fig. 4 and Fig. 5, respectively. The inflow velocity was kept at 10 m/s and the rotational speed was varied to obtain the results for the tip speed ratios of λ= 2, 4, 5, 6, 7, 9 and 11 as employed in the wind tunnel tests. As it can be seen from these figures, the C_p - λ curves are close to the experimental results. Both the k-ε Realizable and *k-ω* SST models show a good performance and the results of both models are very close to each other. The *k-ε* Realizable turbulence model was better at predicting the power coefficient since the k-ω SST turbulence model over predicted the power coefficient at higher tip speed ratios. Also the power coefficient results for the k-ω SST model are similar to the results given by Krogstad and Lund (2012). The behaviour of the C_t – λ curve is similar to the experimental curve and the CFD results appear to under predict the thrust forces, especially at higher tip speed ratios, however one should note that the thrust on the tower is not considered in the CFD calculations. For the simulation of wind turbines with swept blades at λ=6, the k-ε Realizable model is employed since it showed the best performance.

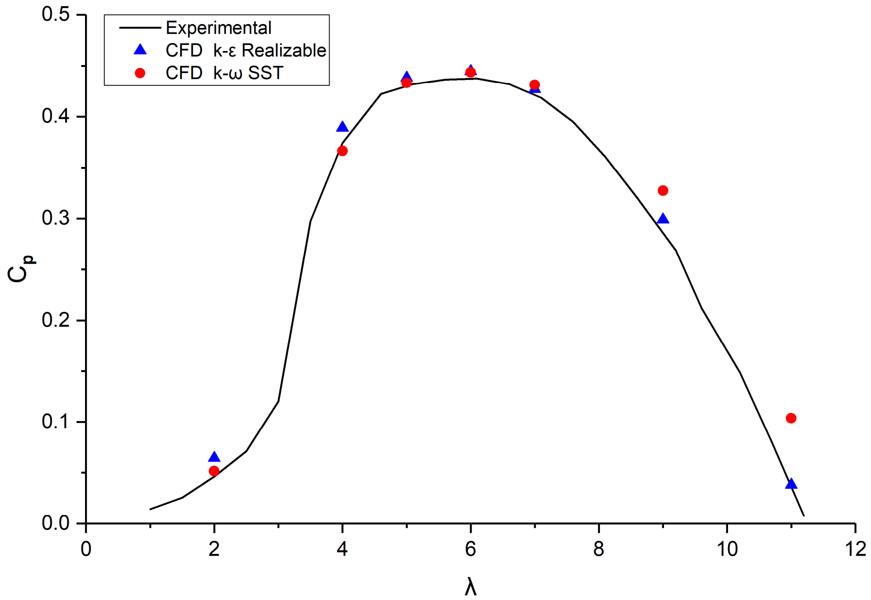

Fig. 4. Comparison of the power coefficient, C_p, as a function of the tip speed ratio, λ, using the experimental data and the CFD results.

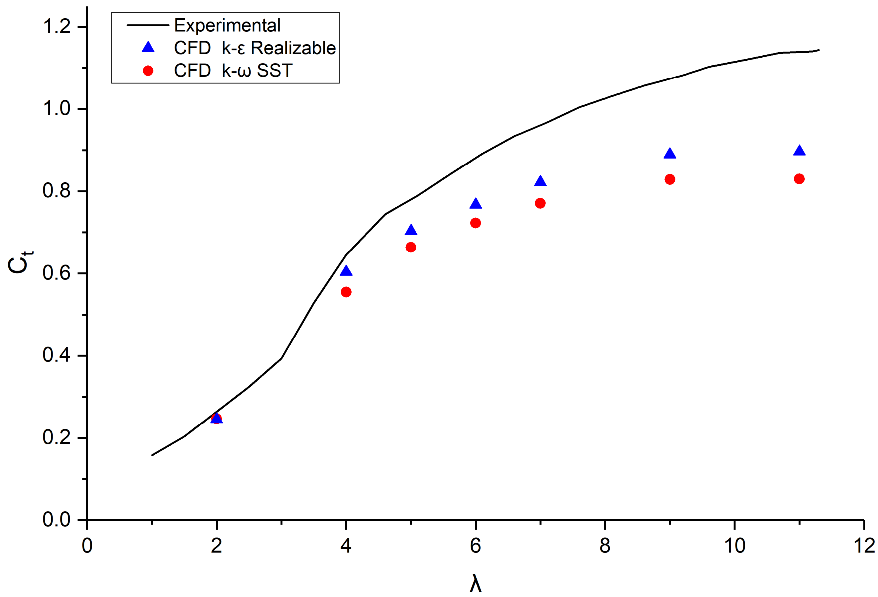

Fig. 5. Comparison of the reaction of the thrust coefficient, C_t, as a function of the tip speed ratio, λ, using the experimental data and the CFD results.

4. Results

In this study, the aerodynamic performances of swept blades are investigated using CFD simulations performed for the design tip speed ratio of 6 at the wind speed of 10 m/s. Changes in the power and thrust coefficients for the wind turbines with swept blades are compared to the values obtained for the baseline wind turbine. To make it easier to understand the results obtained, a method that defines the swept blades is developed. In this method, two indices, i.e. f for forward and b for the backward, are used as the first letter to define the direction of the sweep. After the first indication letter, the first two digits are used to define the ratio of the location of the sweep start section (d/R) to the blade length and the next two digits are used to define the blade tip offset (r_{ss}/R), e.g. “f1510” indicates the forward swept blade which has sweep start at 15% of the span (r_{ss}/R=0.15) and which has 10% (d/R=0.10) offset at the tip.

As stated before, the simulation results obtained using the k-ε Realizable turbulence model was used for the comparison figures in the result section since it was most successful CFD model in the validation. In Fig. 6, surface plots that show the changes in the power coefficients (C_p) and thrust coefficients (C_t) of the wind turbines with forward and backward swept blades compared to the baseline wind turbine. As it can be seen from the figure, there are improvements in the aerodynamic performance for wind turbines with some swept blades compared to the baseline case. The wind turbine with the swept blade “f1520” has the highest performance increase with a value of almost 2.9%. Also, it can be observed that the power output does not increase for every forward swept blade. The thrust coefficients mostly decreases for the wind turbines with backward swept blades and this causes a drop in power performance. It should be noted that for the wind turbine with the swept blade “f1520” there was a smaller increase in thrust coefficient compared to the power coefficient. The changes in power and thrust coefficients appear to be similar for the backward swept blades, especially for those with smaller sweep start up sections. It is clear from the surface plots that increase in power production is obtained in forward swept blades that have smaller sweep start up sections and higher tip displacements.

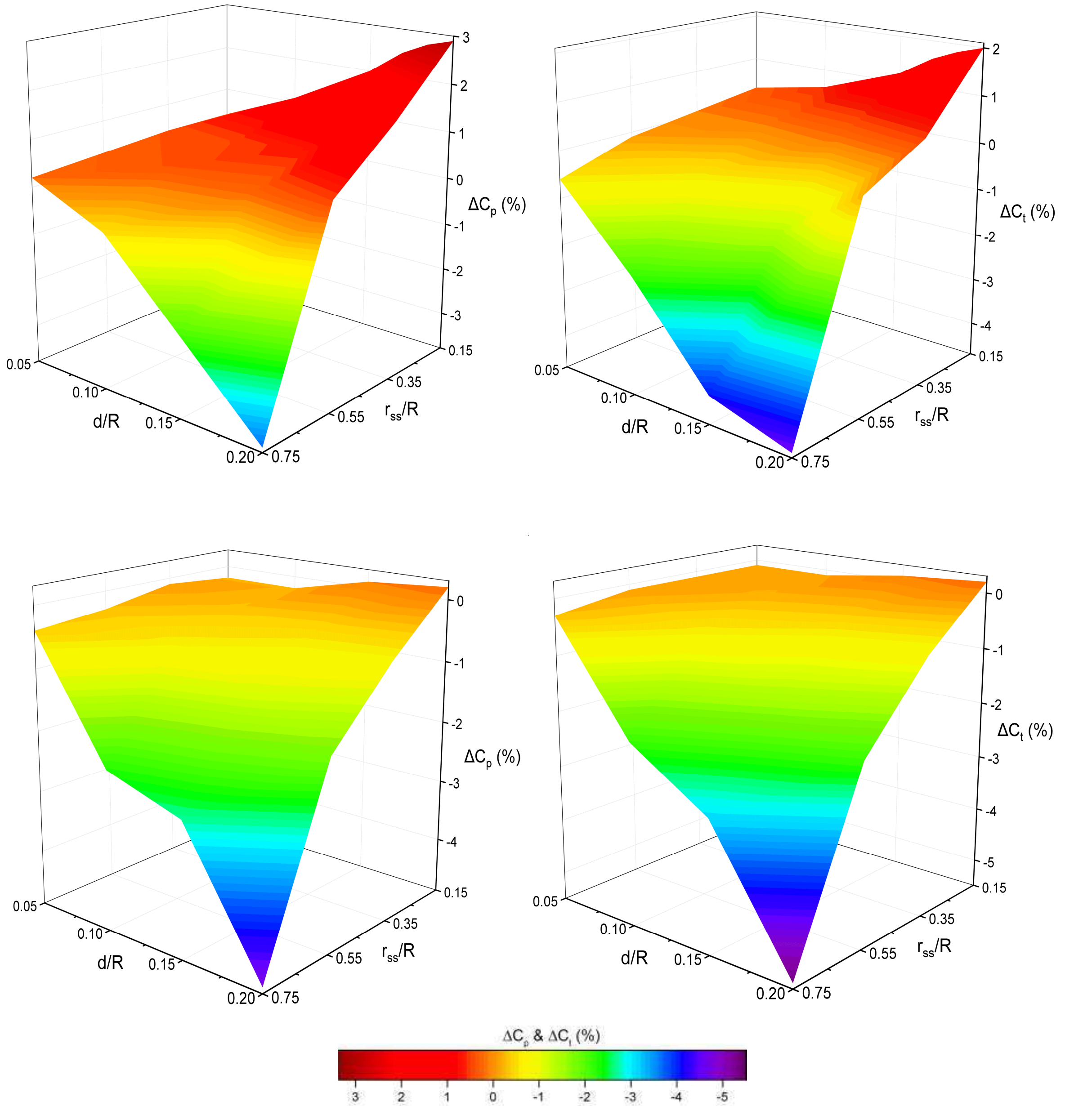

Fig. 6. Surface plots showing the change in C_p and C_t for the forward (top) and backward (bottom) swept blades according to sweep start section (r_{ss}/R) and tip displacement (d/R).

Fig. 7 and Fig. 8 compare the C_p - λ and C_t – λ curves for the baseline and the most efficient design and it is observed that there is an increase in the power coefficient at almost all tip speed ratios. As expected, the increase in the power coefficient has a cost, namely an increase in the thrust coefficient.

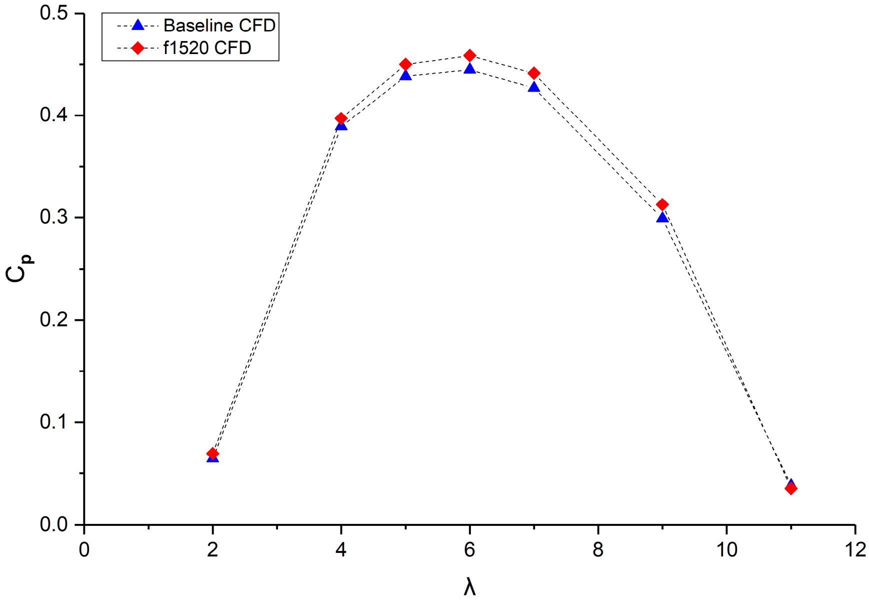

Fig. 7. Comparison of the C_p – λ curves for the baseline and most efficient design.

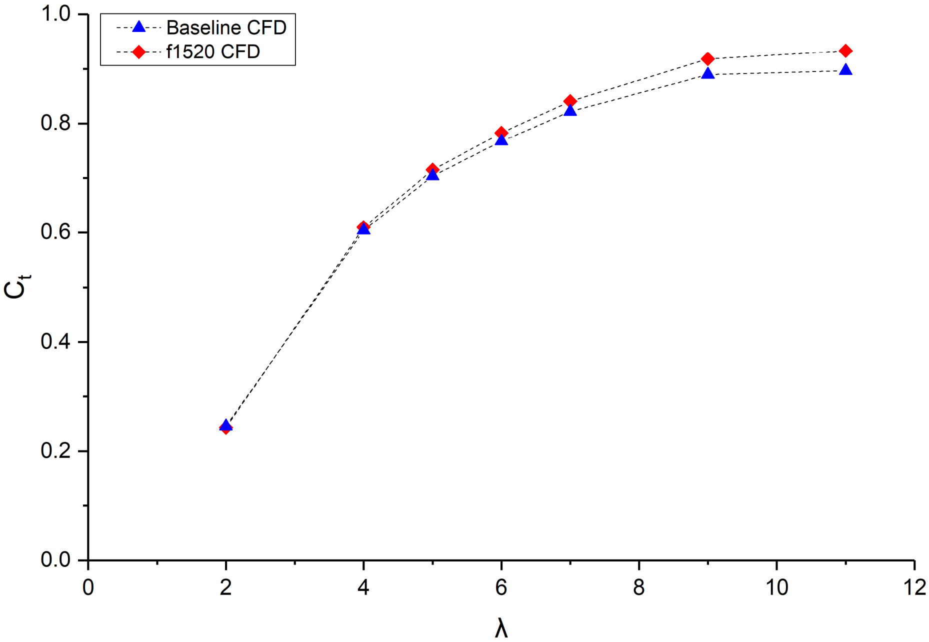

Fig. 8. Comparison of the C_t – λ curves for the baseline and most efficient design.

The pressure distributions for the baseline and the most efficient designs are compared for four sections of the blade, r/R=0.25, 0.50, 0.80 and 0.95, in Fig. 9. As it can be observed, f1520 has a slightly higher pressure difference between the suction and pressure sides at each given section along the blade compared to the baseline. The difference is clearer from the leading edge to the section at x/c=0.4. Since the area integral over the closed pressure coefficient curve is the lift coefficient of the section, a larger area leads to a higher lift (Al-Abadi, 2014).

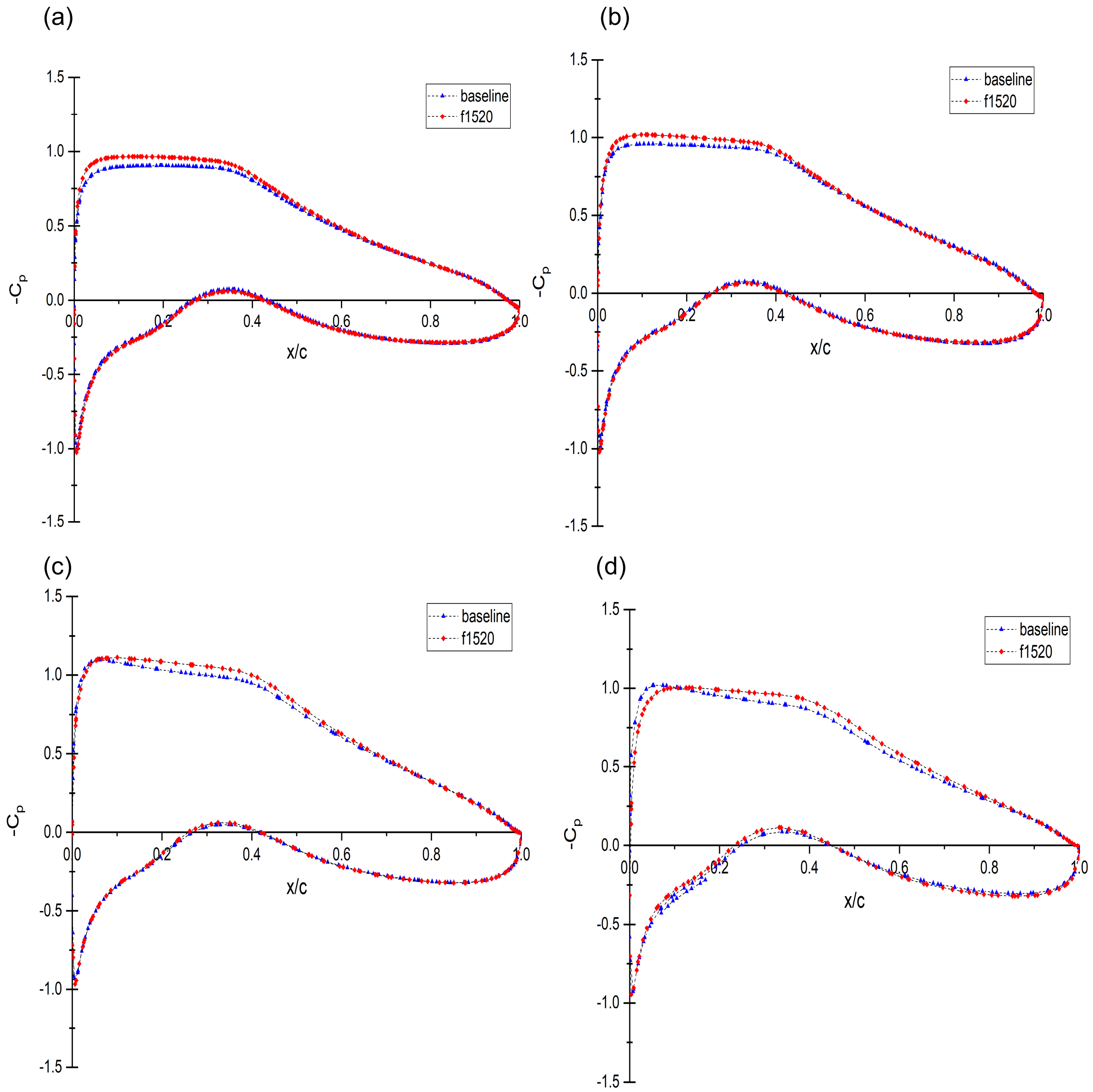

Fig. 9. Pressure distribution comparisons at (a) r/R=0.25; (b) r/R=0.5, (c) r/R=0.80 and (d) r/R=0.95.

One reason for the increase in the power coefficient could be the increase in the flow stream around the blade (Khalafallah, 2015; Sairam and Turner, 2014). According to Sairam and Turner (2014), the radial force variations play a dramatic role in the wind turbine performance since the radial force variation creates streamline curvature that expands the stream tube which causes the wind to slow down near the leading edge of the blade. The radial force distributions are compared for the f1520 and baseline blades in Fig. 10 (a) and the observed data verify the previous statement, and f1520 has mostly a negative radial force distribution whereas the baseline blade has a positive radial force distribution. In Fig. 10 (b), streamwise force distributions on the blades are compared and as it can be observed from the figure, the curves are very similar for both blades except that there is a small difference near the tip. As for the tangential force distributions on the blades, Fig. 10 (c), the f1520 has clearly a higher tangential force in most of the blade sections, especially between r/R=0.2 and r/R=0.5.

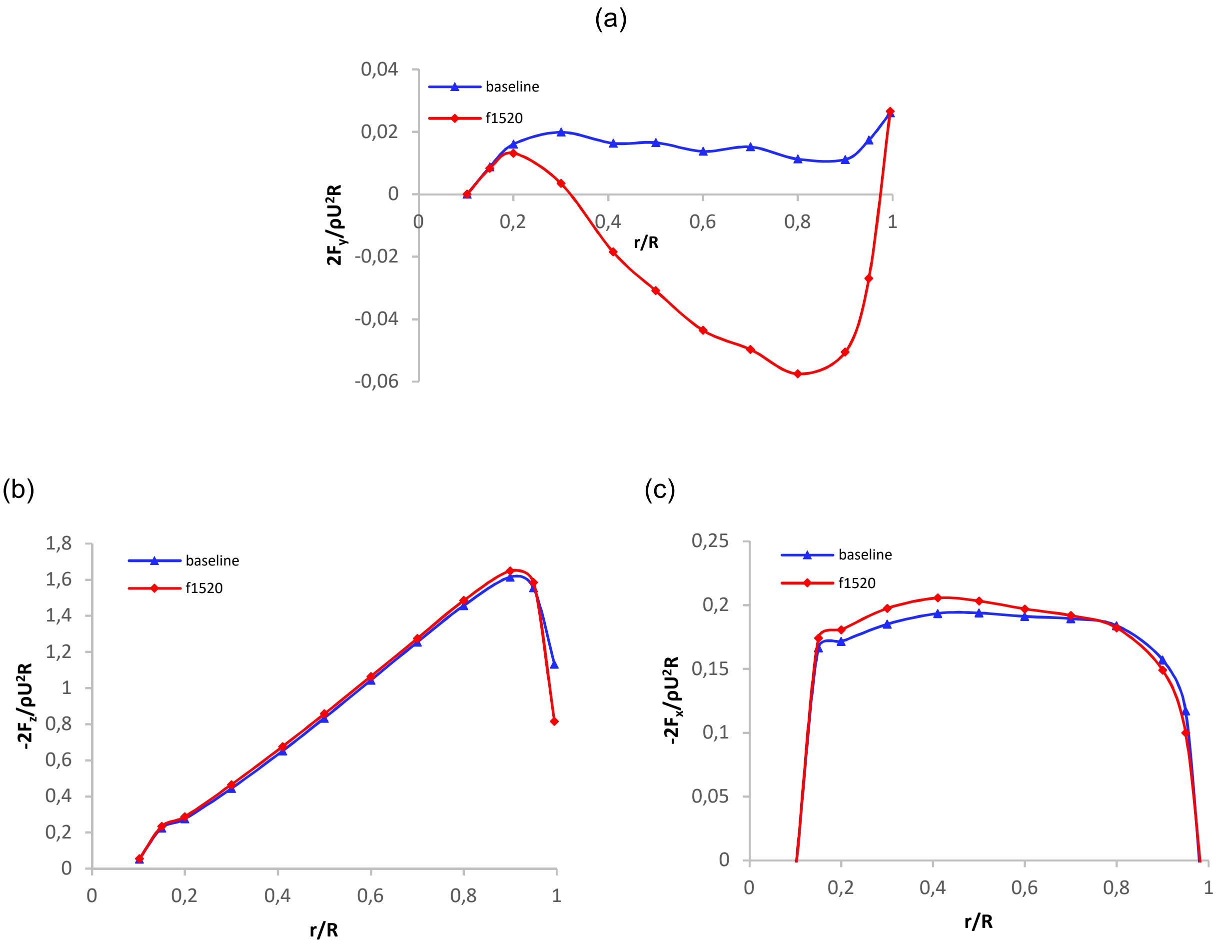

Fig. 10. Dimensionless (a) radial force, F_y, (b) streamwise force, F_z, and (c) tangential force, F_x, distributions along the span of the baseline and f1520 blades.

Finally, Fig. 11 shows iso-surfaces of the vorticity magnitude (top $\omega = 70\ s^{-1}$, bottom $\omega = 2500\ s^{-1}$) and contours of the vorticity at a quarter tip chord downstream of the blades for the baseline (left) and f1520 (right) blades. It is observed from the figure that the blade tip vortices are similar for both blades; however, the tip vortex for the f1520 blade appears to be slightly less intense.

5. Conclusion

This study investigates the aerodynamic performances of horizontal axis wind turbines with forward and backward blades using the NTNU wind turbine as a baseline. CFD simulations are performed for the wind turbines that have four sweep start locations and four offset values. The highest power performance improvement has been obtained for the wind turbine with the forward swept blade that has sweep start up at $r_{ss}/R=0.15$ and tip offset of $d/D=0.2$ (f1520) showing an increase in the power coefficient of about 2.9%. The highest drop in the thrust coefficient is obtained with the backward swept blade that has sweep start up at $r_{ss}/R=0.75$ and tip displacement of $d/D=0.2$ (b7520). Overall, more power is obtained for the forward swept blades with smaller sweep start up sections and higher tip offset values. In conclusion, performance improvement can be made with forward swept blades while a reduction in thrust coefficient could be obtained using the backward swept blades.

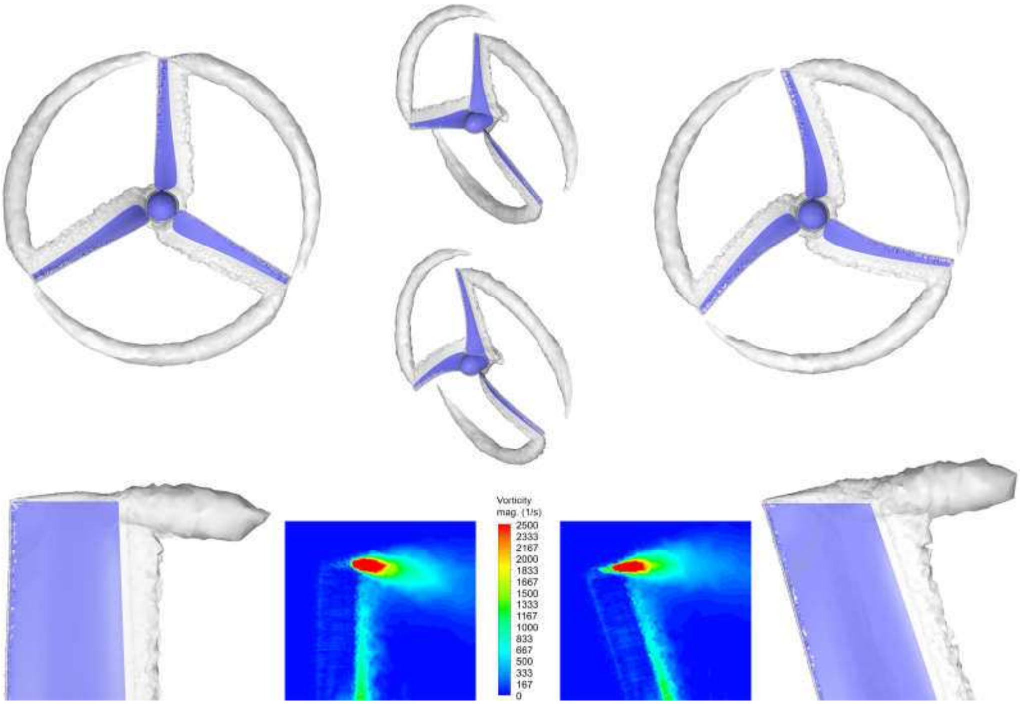

Fig. 11. Iso-surfaces of vorticity magnitude (top ω = 70 s^{-1}, bottom ω = 2500 s^{-1}) and contours of vorticity magnitude for the baseline (left) and f1520 (right) blades.

ACKNOWLEDGEMENT

Mehmet Numan Kaya would like to thank to TÜBİTAK (The Scientific and Technological Research Council of Turkey) for granting him a national and international PhD fellowship during his PhD studies. This work prepared as a part of his PhD study.

Nomenclature

C_p	power coefficient
C_t	thrust coefficient
b	backward
f	forward
F_x	local force per unit width in the tangential direction
F_y	local force per unit width in the radial direction
F_z	local force per unit width in the streamwise direction
M	mode (strength) of the sweep
P_s	ratio of the tip offset to the blade radius ($P_s = d/R$)
P_r	ratio of the radial distance to the blade radius ($P_r = r_r$/R)
P_{rss}	ratio of the radial distance of the sweep start up to the blade radius ($P_{rss}=r_{ss}/R$)
R	blade radius
r_{ss}	radial distance of the sweep start section
r_r	radial distance of the section
ω	vorticity

z_{offset} offset of the blade section from the pitchline

$z_{offset,tip}$ offset at the tip of the blade ($z_{offset,tip} = R \times P_s$)

λ tip speed ratio

REFERENCES

Al-Abadi A., 2014. Novel Strategies for Aerodynamic Performance Improvement of Wind Turbines in Turbulent Flow, PhD thesis, Friedrich-Alexander-University-Erlangen-Nurnberg, Germany.

Amano, R., Avdeev I., Malloy R., Shams M. Z., 2013. Power, Structural and Noise Performance Tests on Different Wind Turbine Rotor Blade Designs. Int. J. Sustainable Energy 32 (2), 78–95.

Ashwill, T., 2010. Sweep-Twist Adaptive Rotor Blade: Final Project Report (No. SAND2009-8037). Sandia National Laboratories.

Ashwill, T., Kanaby G., Jackson K., Zutech M., 2010. Development of the Swept Twist Adaptive Rotor (STAR) Blade. 48th AIAA Aerospace Sciences Meeting, Orlando, FL.

Bai, C. J., Hsiao, F.B., Li, M.H., Huang, G.Y., Chen, Y.J, 2013. Design of 10 kW Horizontal-Axis Wind Turbine (HAWT) Blade and Aerodynamic Investigation Using Numerical Simulation. Procedia Eng. 67, 279-287.

Chattot, J.J., 2009. Effects of blade tip modifications on wind turbine performance using vortex model. Computers & Fluids 38 (7), 1405-1410.

Elfarra, M. A., Sezer-Uzol, N., Akmandor, I. S., 2014. NREL VI rotor blade: numerical investigation and winglet design and optimization using CFD. *Wind Energy*, *17*(4), 605-626.

Hansen, M. H., 2011. Aeroelastic Properties of Backward Swept Blades. 49th AIAA Aerospace Sciences Meeting including the New Horizons Forum and Aerospace Exposition.Orlando, Florida.

IRENA, 2012. Renewable Energy Technologies: Cost Analysis Series: Wind Power. Volume 1 5/5.

Jafari S.A.H., Kosasih B., 2014. Flow analysis of shrouded small wind turbine with a simple frustum diffuser with computational fluid dynamics simulations. J. Wind Eng. Ind. Aerodyn. 125, 102-110.

Karthikeyan, N., Kalidasa, Murugavel, K., Arun, Kumar, S., Rajakumar, S., 2015. Review of aerodynamic developments on small horizontal axis wind turbine blade. Renewable Sustainable Energy Rev. 42, 801-822.

Khalafallah, M.G., Ahmed A.M., Emam M.K. 2015. CFD study of some factors affecting performance of HAWT with swept blades. Int. J. Sustainable Energy 36 (5), 489-501.

Krogstad, P.-A., Lund, J.A., 2012. An experimental and numerical study of the performance of a model turbine. Wind Energy 15, 443–457.

Larin P., Paraschivoiu P., Aygun C., 2016. CFD based synergistic analysis of wind turbines for roof mounted integration. J. Wind Eng. Ind. Aerodyn. 156, 1-13.

Lee M-H., Shiah Y.C., Bai C-J., 2016. Experiments and numerical simulations of the rotor-blade performance for a small-scale horizontal axis wind turbine. J. Wind Eng. Ind. Aerodyn. 149, 17-29.

Moshfeghi M., Shams S., Hur N., 2017. Aerodynamic performance enhancement analysis of horizontal axis wind turbines using a passive flow control method via split blade, J. Wind Eng. Ind. Aerodyn. 167, 148-159.

Pierella, F., Krogstad P.-A., Sætran L., 2014. Blind Test 2 calculations for two in-line model wind turbines where the downstream turbine operates at various rotational speeds. Renew. Energy 70, 62-77.

REN21, 2017. Renewables 2017 Global Status Report. Paris.

Sairam, K., Turner M. G., 2014. The Influence of Radial Area Variation on Wind Turbines to the Axial Induction Factor. Energy Power Eng. 6, 401–418.

Shen X., Yang H., Chen J., Zhu X., Du Z., 2016. Aerodynamic shape optimization of non-straight small wind turbine blades, Energy Convers. Manage. 119: 266-278..

Sørensen NN, Michelsen JA, Schreck S. 2002. Navier–Stokes predictions of the NREL Phase VI rotor in the NASA Ames 80-by-120 wind tunnel AIAA, AIAA-2002-0031.

Verelst, D. R. S., Larsen, T. J., 2010. Load Consequences When Sweeping Blades-A Case Study of a 5 MW Pitch Controlled Wind Turbine. Risø-R-1724, Roskilde: Riso National Laboratory.